

Ancient Monuments Laboratory
Report 45/93

ARCHAEOMAGNETIC DATING:
ST PETER'S CHURCH,
EYNHAM, OXFORD

N Linford

AML reports are interim reports which make available the results of specialist investigations in advance of full publication. They are not subject to external refereeing and their conclusions may sometimes have to be modified in the light of archaeological information that was not available at the time of the investigation. Readers are therefore asked to consult the author before citing the report in any publication and to consult the final excavation report when available.

Opinions expressed in AML reports are those of the author and are not necessarily those of the Historic Buildings and Monuments Commission for England.

Ancient Monuments Laboratory Report 45/93

ARCHAEOLOGICAL DATING:
ST PETER'S CHURCH,
EYNHAM, OXFORD

N Linford

Summary

During an excavation on the site of St Peter's Church, Eynham, three distinct areas of burnt stone were discovered and subsequently sampled for archaeological dating. The features produced results suggesting that the hearths formed a chronological series dating from the Saxon period onwards.

Author's address :-

N Linford

Ancient Monuments Laboratory
English Heritage
23 Saville Row
London
W1X 1AB

Archaeomagnetic Dating: St Peters Church, Eynsham, Oxford.

Introduction

During an excavation by the Oxford Archaeological Unit on the site of Eynsham Abbey at St Peters Church, Eynsham, three distinct areas of burnt stone were discovered which were thought to be hearths dating from the Saxon period onwards.

The three features (site codes 1178, 1184 and 1216) were sampled for archaeomagnetic dating and assigned the AML codes of 1EYN, 2EYN and 3EYN respectively. Feature 1EYN was superimposed upon feature 2EYN and therefore assumed to be of a later date. Sampling of all the features was carried out on the 11th March 1991 by P Linford of the Ancient Monuments Laboratory.

Method

Samples were collected using the disc method (see appendix, section 1a) and orientated to true north with a gyro-theodolite. Seven samples were successfully recovered from feature 1EYN, eighteen from sample 2EYN and twelve from sample 3EYN. Their composition was as follows:

1EYN04, 1EYN08-1EYN12 and 1EYN15: Burnt sandstone.

2EYN01-2EYN18: Burnt sandstone/limestone.

3EYN01: Pink brick.

3EYN04-3EYN07: Red/grey burnt sand.

3EYN08 and 3EYN10: Grey brick.

3EYN11-3EYN15: Burnt sandstone.

Results

All the measurements discussed below were made using the equipment described in section 2 of the appendix; the corrections discussed in sections 3b and 3c of the appendix have been applied.

Feature 1EYN

The natural remanent magnetisation (NRM) of the samples from this feature are tabulated in Table 1 and a graphical representation of these directions is depicted in Figure 1. Samples 1EYN04 and 1EYN08 are not included in the figure as both exhibited a very low intensity magnetisation. The distribution of the NRM directions of the remaining samples is highly scattered. No correlation can be observed between the NRM directions of samples taken from adjacent areas of the hearth; it is thus unlikely that disturbance of the feature

since its last firing is the primary cause of the anomalous scattering. One sample, 1EYN11, has a much lower intensity than the others suggesting a marked variation in the uniformity of heating above the blocking temperature.

The mean thermoremanent direction (see appendix 3d) was calculated from these results and is depicted graphically, superimposed on the calibration curve (see appendix section 4a), in Figure 2. The mean direction is:

**Dec = 14.470 +/- 5.033°; Inc = 60.534 +/- 2.476°;
Alpha-95 = 5.243°;**

The date range derived from this mean is:

**1169 - 1239 cal AD at the 68% confidence level.
1131 - 1265 cal AD at the 95% confidence level.**

Despite a plausible correspondence with the calibration curve the precision of this mean, as indicated by the Alpha-95 statistic, is unacceptably poor resulting in a wide error bar for the date range. Whilst it is unlikely that a mean of high precision will be obtained from a distribution of only 5 samples, three possible reasons for the particularly poor precision can be advanced:

- 1) The feature has been disturbed since the firing event.
- 2) An unstable viscous component in the magnetisation is corrupting the NRM direction.
- 3) The material was not heated sufficiently to cause the complete realignment of the magnetic domains.

To investigate the stability of remanence, a pilot sample, 1EYN15, was partially demagnetised in 2mT increments, to a maximum of 40mT (see appendix, section 2b). Measurements of the remaining remanent magnetisation at each stage are tabulated in Table 2. The decline in intensity of magnetisation with increasing AF demagnetisation is plotted in Figure 3; the variation in the remanent direction is depicted in Figure 4.

Inspection of figure 3 shows a flattened, inverse "S" curve with one suspect measurement, at 20mT, possibly due to instrument error. The steepness of this curve at low coercivity values shows that a higher than expected proportion of magnetic remanence is concentrated in the smaller magnetic domains. It is likely that this is due to viscous remanence acquired since the last firing of the hearth.

Examination of Figure 4 is obscured by the behaviour of the direction of magnetisation at high values of AF demagnetisation; hence, a second plot, showing only measurements up to 18mT is included as Figure 5. Inspection of the latter reveals that the thermoremanent direction is most stable between 6mT and 10mT; it was thus decided to partially demagnetise the rest of the samples in an 8mT AF field, the centre of this range. Measurements of the remaining thermoremanent magnetisation in each sample after this

treatment are tabulated in Table 3 and their distribution is shown in Figure 6. Corrections were made to the measurements according to sections 3b and 3c of the appendix.

The distribution of thermoremanent directions in Figure 6 has been tightened into a more convincing, but still loosely scattered group. However the directions of samples 1EYN04 and 1EYN08 continued to lie well beyond the calibration curve and were therefore excluded from further calculation. The mean thermoremanent direction of the partially demagnetised samples is illustrated graphically in Figure 7 and was calculated to be:

Dec = 14.238 +/- 3.311°; Inc = 61.269 +/- 1.591°;
Alpha-95 = 3.366°

This mean is in a slightly different position to the mean of the NRM results and a higher degree of precision indicated by the Alpha-95 statistic. The date range derived from this mean is:

1175 - 1222 cal AD at the 68% confidence level.
1150 - 1244 cal AD at the 95% confidence level.

These date ranges should be treated with some caution as they are based on a mean direction derived from only five samples.

Feature 2EYN

The NRM results from this feature are tabulated in Table 4 and shown graphically in Figure 8. Samples 2EYN02, 2EYN04 and 2EYN18 were removed from consideration since their directions lay well away from any point on the calibration curve: probably due to these parts of the feature being disturbed. Inspection of Figure 8 shows that whilst there are a number of outliers, the thermoremanent directions of most samples form a loose group centred around Dec 20, Inc 65. The mean thermoremanent direction is plotted in Figure 9 and was calculated to be:

Dec = 18.131 +/- 4.434°; Inc = 65.058 +/- 1.870°;
Alpha-95 = 3.433°

The Alpha-95 statistic for this mean indicates a relatively disappointing degree of precision, no doubt attributable to the variance in the distribution of the samples. Examination of the sampling regime indicates that the NRM directions in the central grouping tended to come from samples to the north of the feature, but provides no criteria for the exclusion of outliers. It is therefore reasonable to assume that the precision of the mean has been affected by the same factors as discussed in Feature 1EYN. The date range ascribed to this mean direction is:

1075 - 1144 cal AD at the 68% confidence level.
1033 - 1175 cal AD at the 95% confidence level.

Sample 2EYN08 was partially demagnetised in 2mT increments, to a maximum of 30mT, to investigate the stability of the remanent magnetism. The results of these measurements are tabulated in Table 5; the decline in intensity with increasing AF demagnetisation is plotted in Figure 10. Comparison of Figure 10 with Figure 3 shows a marked similarity in the shape of the curves with an anomalously large proportion of the remanent magnetisation being held by low coercivity domains.

The variation of the remanent direction is plotted in Figure 11 and is most stable between 4mT and 12mT; suggesting that an 8mT partial demagnetisation, the centre of this range, may increase the precision of the mean if applied to the other samples. Thus the remaining samples were partially demagnetised in an 8mT demagnetising field and measurements of their magnetic remanence after this treatment are tabulated in Table 6; the distribution of remanent directions is plotted in Figure 12. The new mean thermoremanent direction, superimposed on the calibration curve, is shown in Figure 13. It can be observed that the partial demagnetisation has preserved the the mean thermoremanent direction but it now shows a slightly lower degree of precision.

**Dec = 18.378 +/- 4.448°; Inc = 63.587 +/- 1.979°;
Alpha-95 = 3.635°**

Corresponding to a date range fractionally earlier than that obtained previously:

**1092 - 1156 cal AD to the 68% confidence level.
1050 - 1188 cal AD to the 95% confidence level.**

Feature 3

The NRM measurements from Feature 3 are tabulated in Table 7 and the directions of remanent magnetism are superimposed upon the calibration curve in Figure 14. Samples 3EYN01, 3EYN04, 3EYN05 and 3EYN06 were excluded since their directions lay well away from the calibration curve; probably as these parts of the feature had been disturbed since last firing. Figure 14 shows four of the remaining samples loosely clustered around the curve, with samples 3EYN07, 3EYN08, 3EYN10 and 3EYN12 forming an anomalous group of outliers. The mean thermoremanent direction of the NRM measurements is shown in Figure 15 and was calculated to be:

**Dec = 33.329 +/- 6.216°; Inc = 62.890 +/- 2.833°;
Alpha-95 = 5.507°**

No date range can be assigned to this mean direction as its 68% ellipse of confidence fails to intersect with the calibration curve.

A pilot demagnetisation of sample 3EYN13 was conducted in 2mT increments, to a maximum of 20mT and the results are tabulated in Table 8. The decline of the remanent magnetisation with increasing AF demagnetisation is plotted in Figure 16 and appears almost linear, suggesting an equal distribution of the magnetic remanence between high and low coercivity domains. The variation of the direction of remanent magnetism is plotted

in Figure 17 and shows an area of stability between 8mT and 12mT; it was thus decided to demagnetise the remaining samples in a 10mT field, the centre of this range. Measurements of the remaining thermoremanent magnetisation in each sample after this treatment are tabulated in Table 9, corrected according to sections 3b and 3c of the appendix; their distribution is shown in Figure 18.

Inspection of Figure 18 shows that after demagnetisation one, 3EYN12, sample lay well away from the calibration curve, probably because it was not heated sufficiently during the firing of the hearth to completely align its magnetic domains. The remaining samples are widely distributed and produce the mean direction depicted in Figure 19. This just grazes the calibration curve with its 68% ellipse of confidence and was calculated to be:

**Dec = 19.917 +/- 5.355°; Inc = 62.015 +/- 2.504°;
Alpha-95 = 4.706°**

The date range corresponding to this mean is:

**1075 - 1169 cal AD at the 68% confidence level.
1000 - 1222 cal AD at the 95% confidence level.**

Owing to the poor precision indicated by the alpha-95 value and the inaccuracy of the mean direction, the date range quoted above should be treated only as a broad indication of the period during which this hearth was last fired.

Conclusion

The three features produced a sequence of date ranges that were in accordance with the excavation evidence:

**Feature 1178: 1175 - 1222 cal AD at the 68% confidence level.
1150 - 1244 cal AD at the 95% confidence level.**

**Feature 1184: 1092 - 1156 cal AD to the 68% confidence level.
1050 - 1188 cal AD to the 95% confidence level.**

**Feature 1216: 1075 - 1169 cal AD at the 68% confidence level.
1000 - 1222 cal AD at the 95% confidence level.**

However, the mean thermoremanent directions from which these date ranges derived were all of poor precision. This is particularly true of the mean of feature 1216 (3EYN), so the date for this feature should be treated simply as an estimation of the broad period during which the last firing occurred. The other two dates should also be treated with caution if other dating evidence does not concur with them.

Partial demagnetisation of the samples indicated that some viscous remanence was corrupting the true thermoremanent directions recorded in the samples. Nevertheless, the poor precision of the mean thermoremanent directions, even after partial demagnetisation, suggests that the hearths were not heated to sufficiently high temperatures during their operation to cause complete realignment of the magnetic domains within the clay that was sampled.

Neil Linford
Archaeometry Branch, SCS/RPSG

8th July 1993

Table 1; Corrected NRM measurements for all samples of Feature 1.

<u>Sample</u>	<u>Declination</u> (deg)	<u>Inclination</u> (deg)	<u>Intensity</u> (Am ² x10 ⁻⁸)
1EYN04	-66.852	-33.121	0.986
1EYN08	-54.651	-64.708	2.945
1EYN09	13.837	59.613	346.652
1EYN10	3.779	66.577	563.115
1EYN11	24.043	55.147	36.541
1EYN12	16.773	59.181	160.707
1EYN15	10.130	61.324	416.498

Table 2; Variation of remanent field with increasing partial demagnetisation for sample 1EYN15.

<u>Demagnetisation</u> (mT)	<u>Declination</u> (deg)	<u>Inclination</u> (deg)	<u>Intensity</u> (M/M ₀)
0	9.442	61.541	1.000
2	9.222	61.670	0.998
4	8.539	61.660	0.977
6	8.398	62.126	0.955
8	8.814	61.867	0.928
10	8.705	61.948	0.888
12	7.544	62.177	0.841
14	8.881	62.214	0.788
16	8.842	62.410	0.734
18	8.430	62.521	0.681
20	9.007	77.762	0.569
22	8.373	62.388	0.577
24	8.796	62.487	0.531
26	7.637	62.461	0.487
28	6.921	62.140	0.445
30	8.361	62.186	0.417
32	7.004	62.427	0.380
34	7.465	62.381	0.348
36	9.061	62.104	0.328
38	6.593	62.494	0.307
40	7.402	62.632	0.290

Table 3; Corrected measurements for all samples of Feature 1 after 8mT AF partial demagnetisation.

<u>Sample</u>	<u>Declination</u> (deg)	<u>Inclination</u> (deg)	<u>Intensity</u> (Am ² x10 ⁻⁸)
1EYN04	4.437	29.943	0.850
1EYN08	13.091	-56.756	1.832
1EYN09	15.564	61.392	317.755
1EYN10	9.587	64.914	478.778
1EYN11	20.514	57.494	34.408
1EYN12	15.296	60.327	141.378
1EYN15	8.814	61.86	393.930

Table 4; Corrected NRM measurements for all samples of Feature 2.

<u>Sample</u>	<u>Declination</u> (deg)	<u>Inclination</u> (deg)	<u>Intensity</u> (Am ² x10 ⁻⁸)
2EYN01	25.798	68.093	289.919
2EYN02	17.516	20.055	11.474
2EYN03	-6.144	70.944	559.224
2EYN04	68.476	78.903	539.048
2EYN05	38.933	74.336	791.942
2EYN06	-6.938	58.635	468.733
2EYN07	5.704	61.802	1028.688
2EYN08	21.309	62.681	1896.324
2EYN09	13.683	60.652	2455.164
2EYN10	21.772	58.620	7034.909
2EYN11	26.371	63.940	2165.123
2EYN12	16.678	64.075	612.180
2EYN13	13.625	62.952	142.586
2EYN14	18.250	68.021	19.645
2EYN15	16.867	62.819	2127.800
2EYN16	38.316	64.263	124.792
2EYN17	36.835	65.396	198.232
2EYN18	63.069	50.845	36.767

Table 5; Variation of remanent field with increasing partial demagnetisation for sample 2EYN08.

<u>Demagnetisation</u> (mT)	<u>Declination</u> (deg)	<u>Inclination</u> (deg)	<u>Intensity</u> (M/M _O)
0	17.119	61.099	1.000
2	17.249	61.123	0.980
4	17.890	61.321	0.953
6	18.287	61.254	0.906
8	18.403	61.111	0.856
10	18.044	60.966	0.798
12	18.382	61.303	0.733
14	17.879	61.080	0.679
16	17.887	60.883	0.606
18	16.881	61.048	0.523
20	16.221	60.881	0.457
22	16.242	60.436	0.395
24	15.875	61.434	0.345
26	17.327	61.364	0.290
28	12.927	61.444	0.244
30	15.678	61.149	0.217

Table 6; Corrected measurements for all samples of Feature 2 after 8mT AF partial demagnetisation.

<u>Sample</u>	<u>Declination</u> (deg)	<u>Inclination</u> (deg)	<u>Intensity</u> (Am ² x10 ⁻⁸)
2EYN01	25.213	68.007	252.535
2EYN02	-31.330	87.293	2.127
2EYN03	-8.523	69.728	472.331
2EYN04	69.455	78.522	391.193
2EYN05	38.634	75.088	531.723
2EYN06	-3.230	57.995	419.531
2EYN07	6.095	62.885	825.605
2EYN08	18.430	61.290	1622.567
2EYN09	16.537	58.459	2264.127
2EYN10	21.725	56.715	6543.735
2EYN11	30.056	61.381	1921.839
2EYN12	19.056	63.546	533.759
2EYN13	12.048	62.251	114.387
2EYN14	14.419	59.242	16.081
2EYN15	17.564	61.779	1894.647
2EYN16	38.111	61.915	106.569
2EYN17	36.531	64.973	178.314
2EYN18	63.799	51.029	34.334

Table 7; Corrected NRM measurements for all samples of feature 3.

<u>Sample</u>	<u>Declination</u> (deg)	<u>Inclination</u> (deg)	<u>Intensity</u> (Am ² x10 ⁻⁸)
3EYN01	50.353	50.384	315.557
3EYN04	52.839	34.742	59.910
3EYN05	62.988	38.009	4346.697
3EYN06	51.628	41.148	1494.086
3EYN07	47.472	55.943	1567.771
3EYN08	43.816	57.369	18.578
3EYN10	44.586	61.782	22.890
3EYN11	17.452	68.746	108.092
3EYN12	36.947	56.582	123.244
3EYN13	20.717	62.802	551.923
3EYN14	23.851	66.218	169.336
3EYN15	17.244	69.578	129.634

Table 8; Variation of remanent field with increasing partial demagnetisation for sample 3EYN13.

<u>Demagnetisation</u> (mT)	<u>Declination</u> (deg)	<u>Inclination</u> (deg)	<u>Intensity</u> (M/M ₀)
0	20.295	63.565	1.000
2	17.431	62.567	0.920
4	12.781	61.496	0.817
6	10.826	60.573	0.715
8	10.358	60.393	0.626
10	11.092	60.196	0.547
12	11.239	59.836	0.462
14	11.946	59.917	0.395
16	12.466	60.023	0.334
18	13.195	59.970	0.283
20	12.731	59.484	0.244

Table 9; Variation of remanent field with increasing partial demagnetisation for sample 3EYN13.

<u>Demagnetisation</u> (mT)	<u>Declination</u> (deg)	<u>Inclination</u> (deg)	<u>Intensity</u> (M/M ₀)
0	20.295	63.565	549.321
2	17.431	62.567	505.497
4	12.781	61.496	448.529
6	10.826	60.573	392.544
8	10.358	60.393	344.094
10	11.092	60.196	300.374
12	11.239	59.836	254.003
14	11.946	59.917	216.896
16	12.466	60.023	183.283
18	13.195	59.970	155.627
20	12.731	59.484	134.165

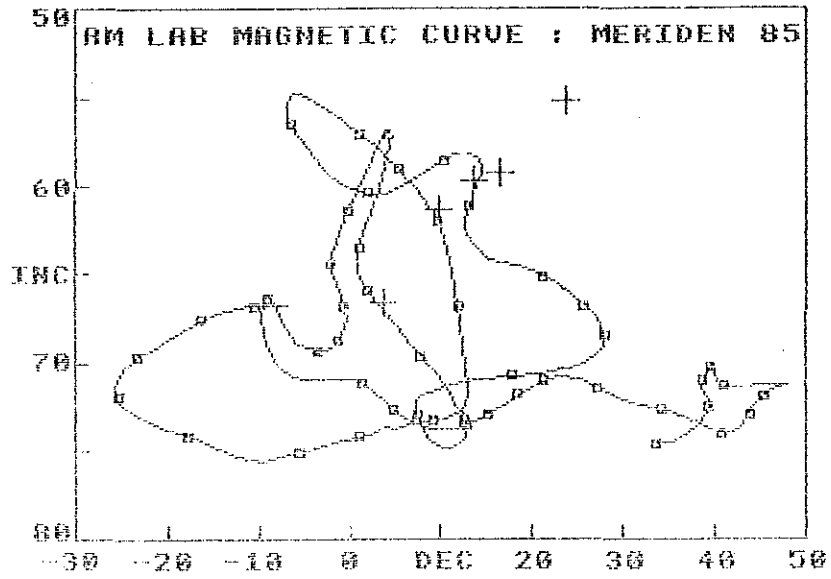


Figure 1; Distribution of NRM results from Feature 1EYN.

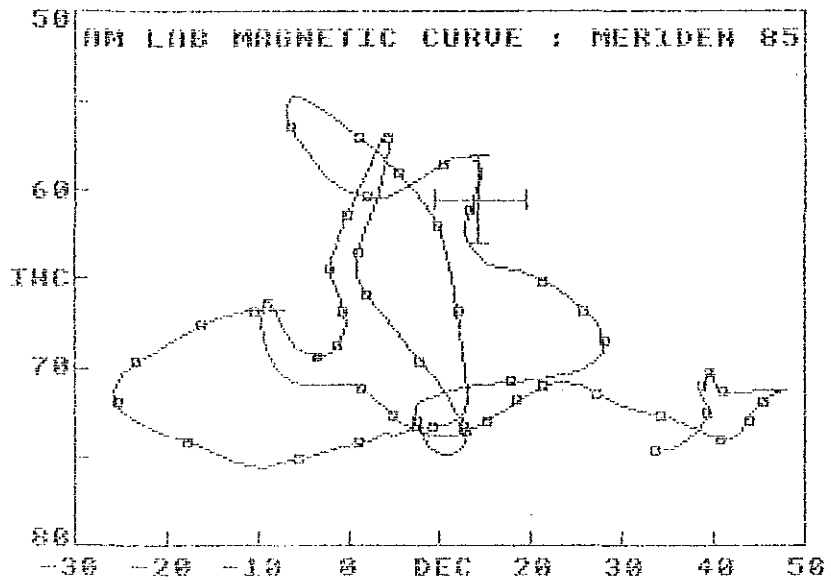


Figure 2; Mean of NRM results from Feature 1EYN with 68% confidence limits.

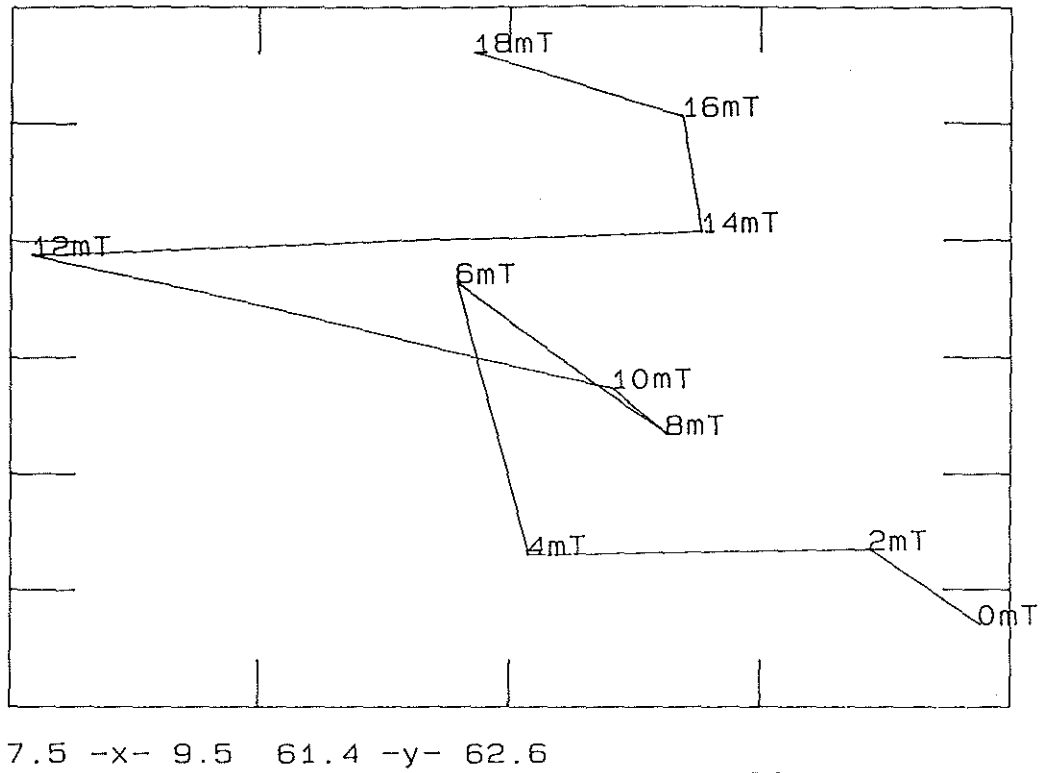


Figure 5; Variation of Dec (x axis) and Inc (y axis) with increasing partial demagnetisation up to 18mT for sample 1EYN15.

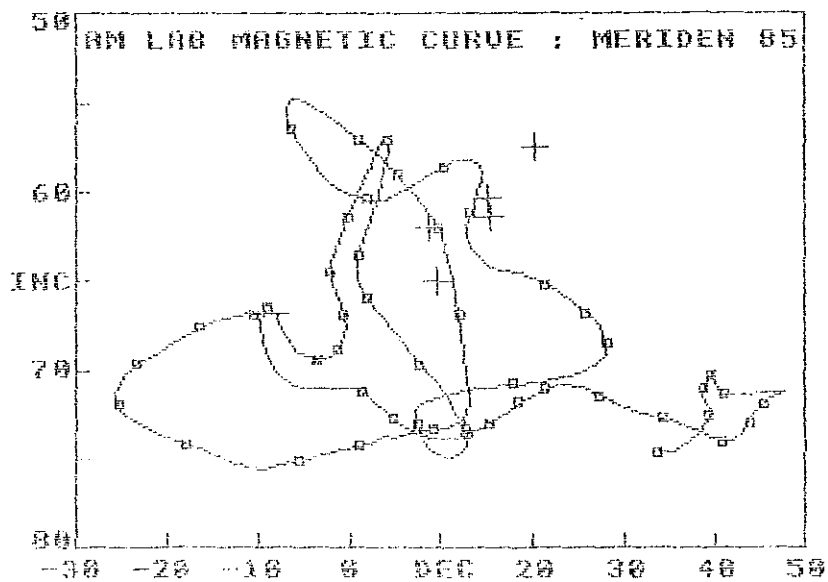


Figure 6; Distribution of partially demagnetised results from Feature 1EYN.

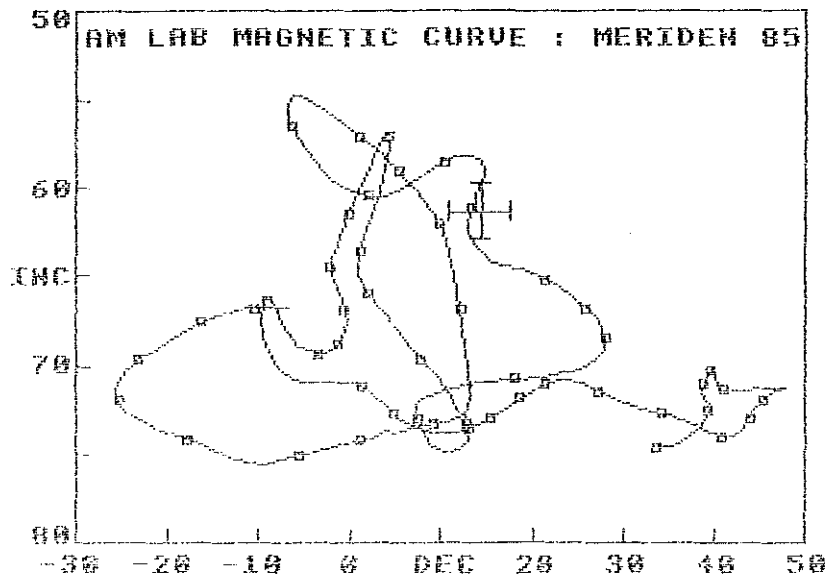


Figure 7; Mean of partially demagnetised results from Feature 1EYN, with 68% confidence limits.

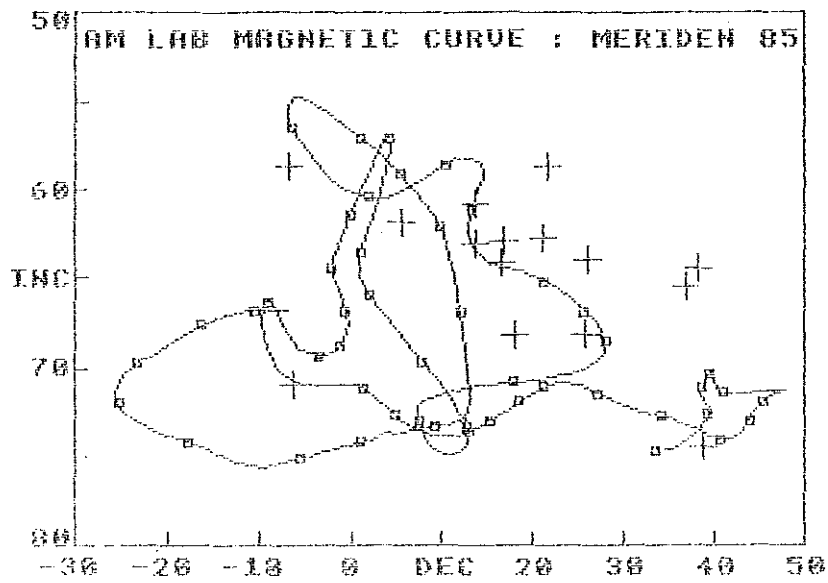


Figure 8; Distribution results of NRM results from Feature 2EYN.

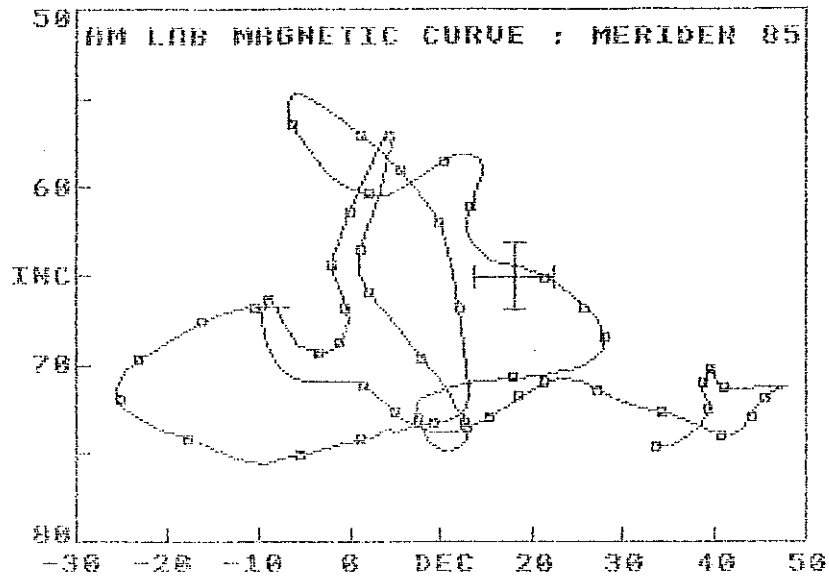


Figure 9; Mean of NRM results from Feature 2EYN.

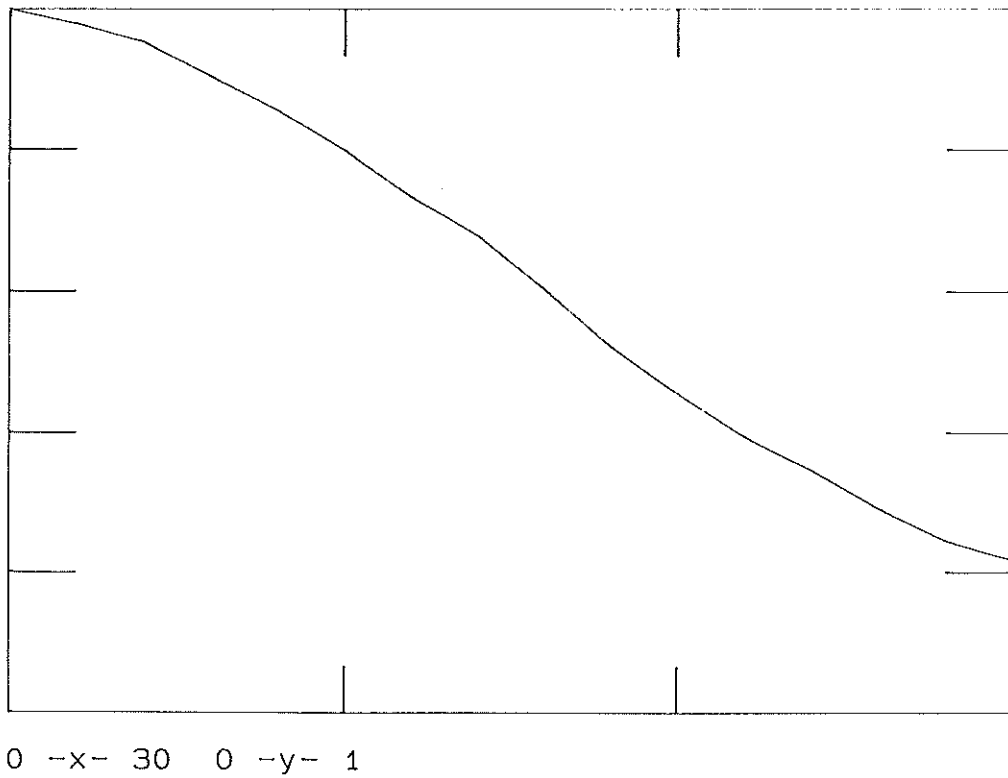
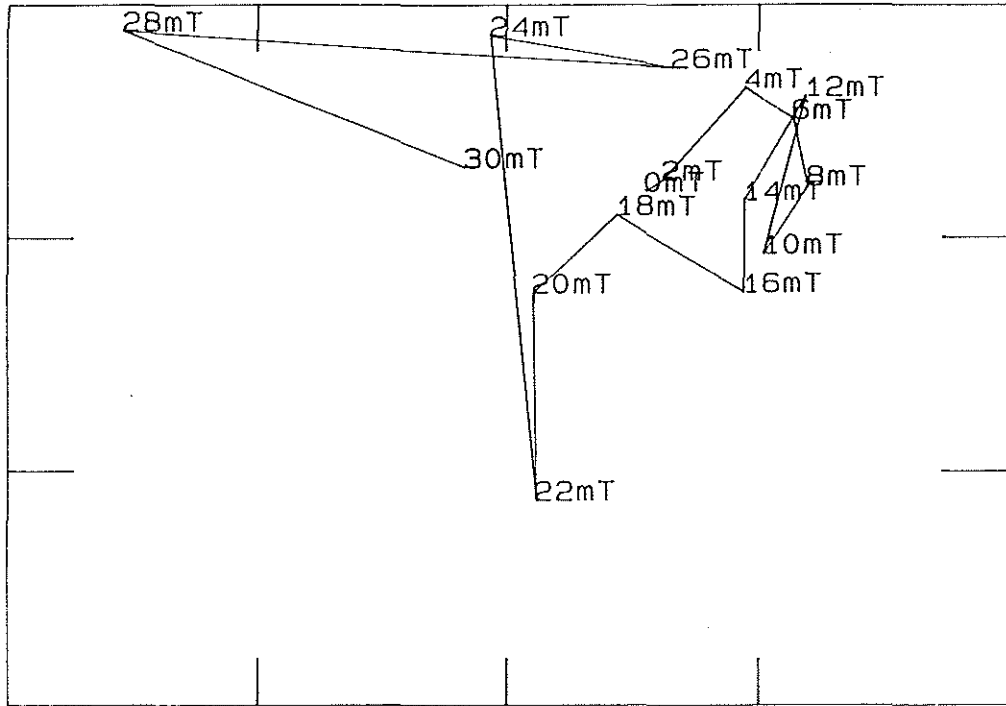


Figure 10; Variation of remanence intensity (y axis), M/M_0 , with increasing partial demagnetisation in mT (x axis), for sample 2EYN08.



12 -x- 20 60 -y- 61.5

Figure 11; Variation of Dec (x axis) and Inc (y axis) with increasing partial demagnetisation for sample 2EYN08.

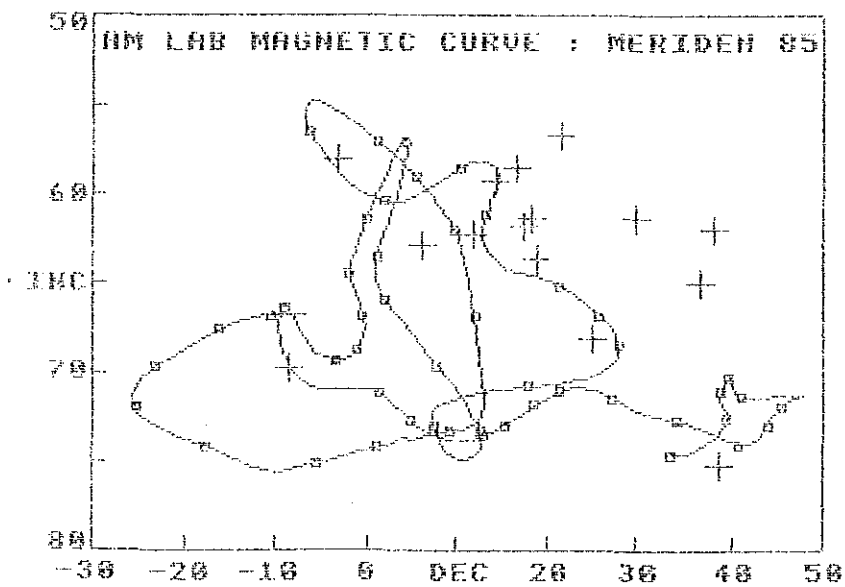


Figure 12; Distribution of partially demagnetised results from Feature 2EYN.

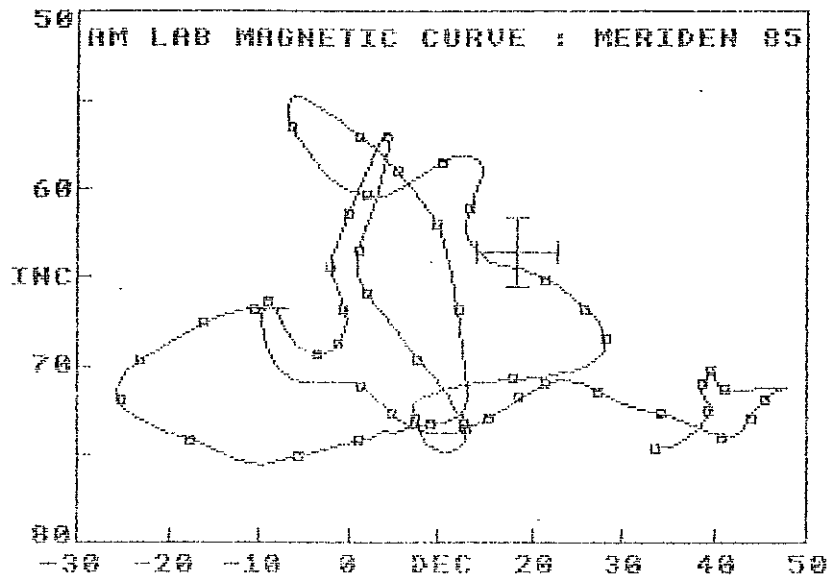


Figure 13; Mean of partially demagnetised results with 68% confidence limits from Feature 2EYN.

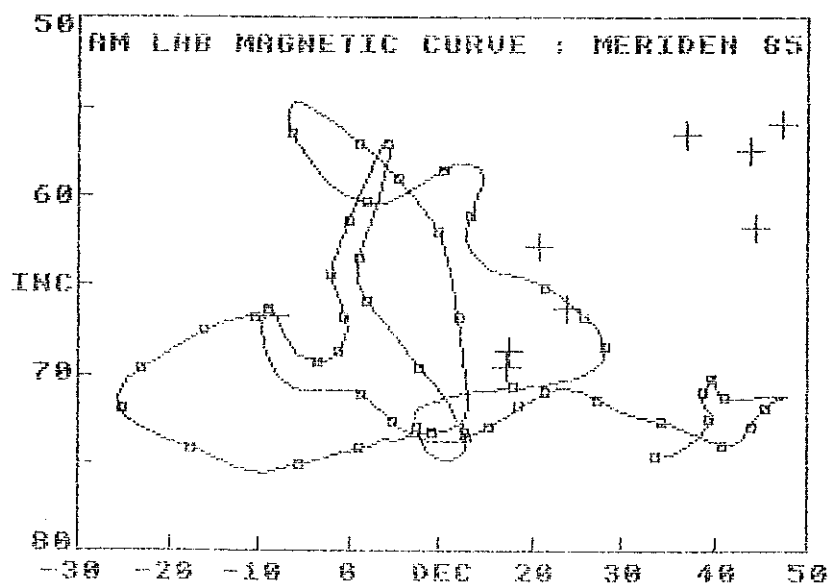


Figure 14; Distribution of NRM results from Feature 3EYN.

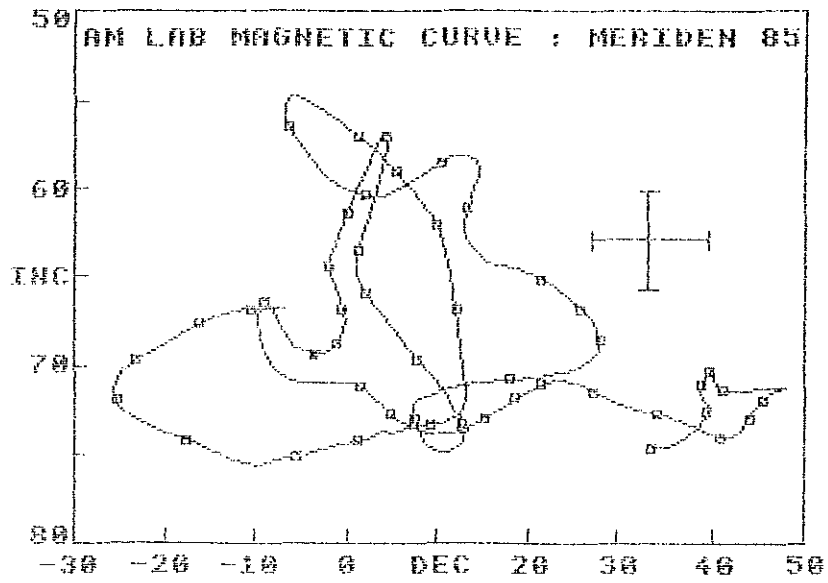


Figure 15; Mean of NRM results from Feature 3EYN with 68% confidence limits.

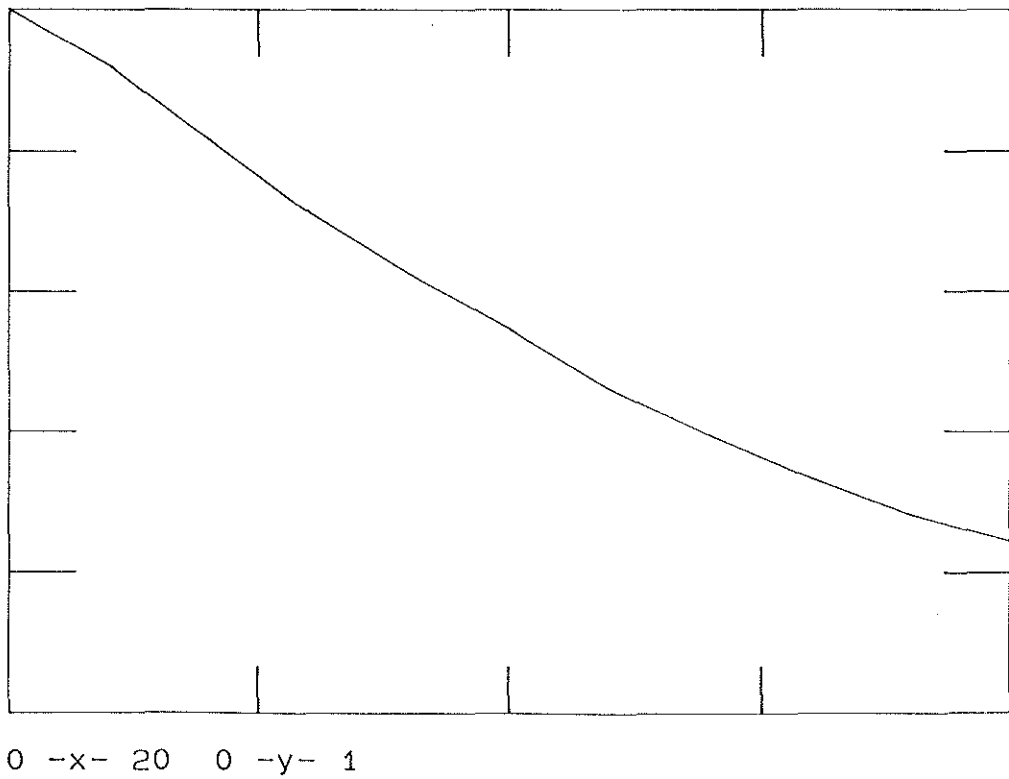
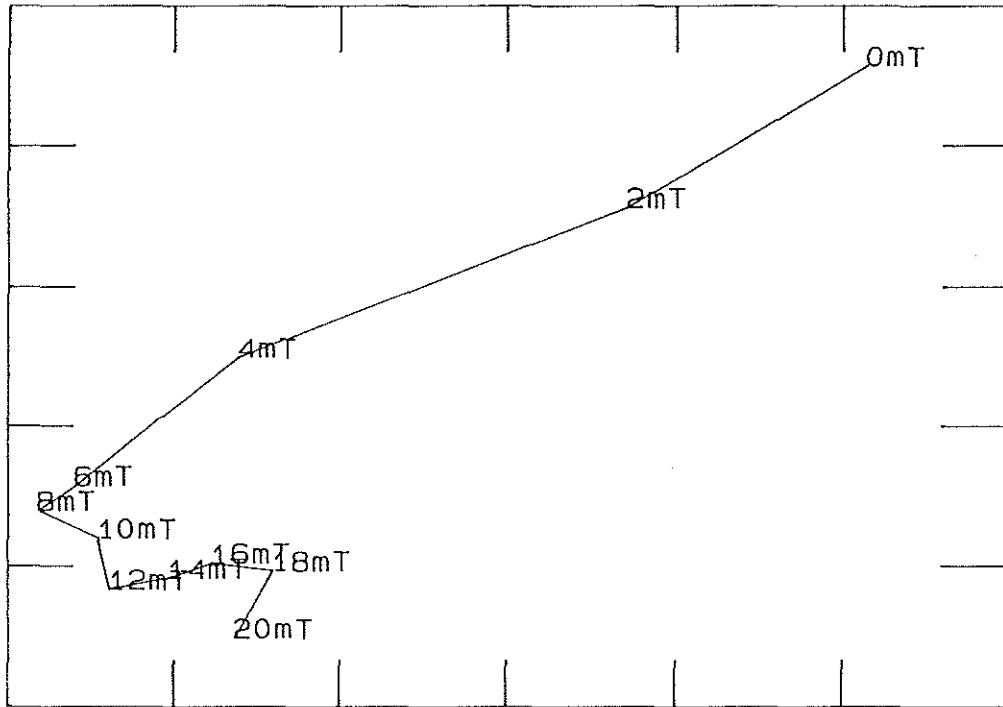


Figure 16; Variation of remanence intensity (y axis), M/M_0 , with increasing partial demagnetisation in mT (x axis), for sample 3EYN13.



10 -x- 22 59 -y- 64

Figure 17; Variation of Dec (x axis) and Inc (y axis) with increasing partial demagnetisation for sample 3EYN13.

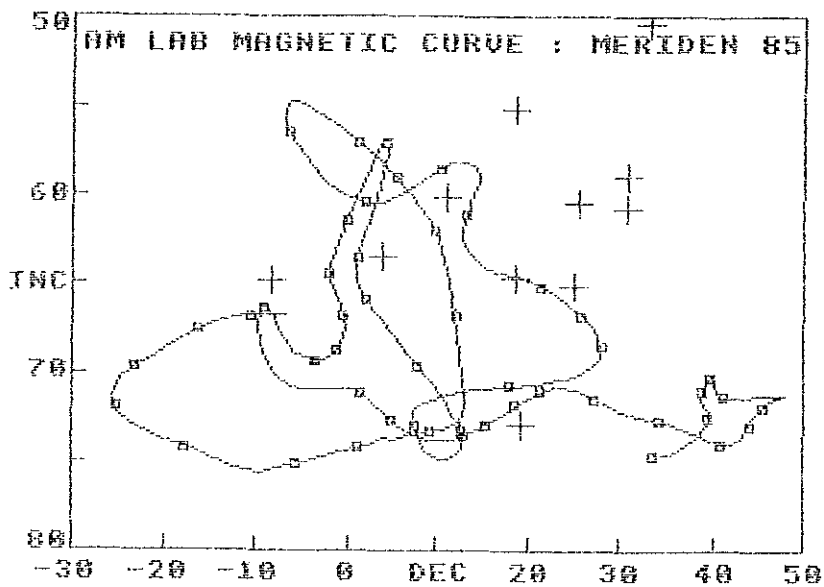


Figure 18; Distribution of partially demagnetised results from Feature 3EYN.

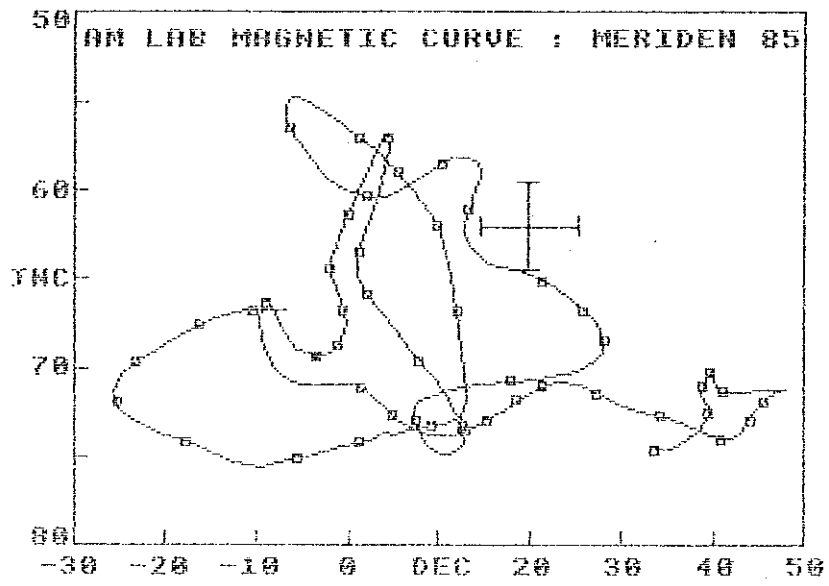


Figure 19; Mean of partially demagnetised results from Feature 3EYN with 68% confidence limits.

Appendix: Standard Procedures for Sampling and Measurement

1) Sampling

One of three sampling techniques is employed depending on the consistency of the material (Clark, Tarling and Noel 1988):

- a) Consolidated materials: Rock and fired clay samples are collected by the disc method. Several small levelled plastic discs are glued to the feature, marked with an orientation line related to True North, then removed with a small piece of the material attached.
- b) Unconsolidated materials: Sediments are collected by the tube method. Small pillars of the material are carved out from a prepared platform, then encapsulated in levelled plastic tubes using plaster of Paris. The orientation line is then marked on top of the plaster.
- c) Plastic materials: Waterlogged clays and muds are sampled in a similar manner to method 1b) above; however, the levelled plastic tubes are pressed directly into the material to be sampled.

2) Physical Analysis

- a) Magnetic remanences are measured using a slow speed spinner fluxgate magnetometer (Molyneux *et al.* 1972; see also Tarling 1983, p84; Thompson and Oldfield 1986, p52).
- b) Partial demagnetisation is achieved using the alternating magnetic field method (As 1967; Creer 1959; see also Tarling 1983, p91; Thompson and Oldfield 1986, p59), to remove viscous magnetic components if necessary. Demagnetising fields are measured in milli-Tesla (mT), figures quoted being for the peak value of the field.

3) Remanent Field Direction

- a) The remanent field direction of a sample is expressed as two angles, declination (Dec) and inclination (Inc), both quoted in degrees. Declination represents the bearing of the field relative to true north, angles to the east being positive; inclination represents the angle of dip of this field.
- b) Aitken and Hawley (1971) have shown that the angle of inclination in measured samples is likely to be distorted owing to magnetic refraction. The phenomenon is not well understood but is known to depend on the position the samples occupied within the structure. The corrections recommended by Aitken and Hawley are routinely applied to measured inclinations, in keeping with the practise of Clark, Tarling and Noel (1988).

- c) Remanent field directions are adjusted to the values they would have had if the feature had been located at Meriden, a standard reference point. The adjustment is done using the method suggested by Noel (Tarling 1983, p116), and allows the remanent directions to be compared with standardised calibration data.
- d) Individual remanent field directions are combined to produce the mean remanent field direction using the statistical method developed by R. A. Fisher (1953). The quantity "alpha-95" is quoted with mean field directions and is a measure of the precision of the determination (see Aitken 1990, p247). It is analogous to the standard error statistic for scalar quantities; hence the smaller its value, the better the precision of the date.

4) Calibration

- a) Material less than 3000 years old is dated using the archaeomagnetic calibration curve compiled by Clark, Tarling and Noel (1988).
- b) Older material is dated using the lake sediment data compiled by Turner and Thompson (1982).
- c) Dates are normally given at the 68% confidence level. However, the quality of the measurement and the estimated reliability of the calibration curve for the period in question are not taken into account, so this figure is only approximate. Owing to crossovers and contiguities in the curve, alternative dates are sometimes given. It may be possible to select the correct alternative using independent dating evidence.
- d) As the thermoremanent effect is reset at each heating, all dates for fired material refer to the final heating.
- e) Dates are prefixed by "cal", for consistency with the new convention for calibrated radiocarbon dates (Mook 1986).

References

- Aitken, M. J. 1990. *Science-based Dating in Archaeology*. London: Longman.
- Aitken, M. J. and H. N. Hawley 1971. Archaeomagnetism: evidence for magnetic refraction in kiln structures. *Archaeometry* **13**, 83-85.
- As, J. A. 1967. The a.c. demagnetisation technique, in *Methods in palaeomagnetism*, D. W. Collinson, K. M. Creer and S. K. Runcorn (eds). Amsterdam: Elsevier.
- Clark, A. J., D. H. Tarling and M. Noel 1988. Developments in Archaeomagnetic Dating in Britain. *J. Arch. Sci.* **15**, 645-667.
- Creer, K. M. 1959. A.C. demagnetisation of unstable Triassic Keuper Marls from S. W. England. *Geophys. J. R. Astr. Soc.* **2**, 261-275.
- Fisher, R. A. 1953. Dispersion on a sphere. *Proc. R. Soc. London A* **217**, 295-305.
- Molyneux, L., R. Thompson, F. Oldfield and M. E. McCallan 1972. Rapid measurement of the remanent magnetisation of long cores of sediment. *Nature* **237**, 42-43.
- Mook, W. G. 1986. Recommendations/Resolutions Adopted by the Twelfth International Radiocarbon Conference. *Radiocarbon* **28**, M. Stuiver and S. Kra (eds), 799.
- Tarling, D. H. 1983. *Palaeomagnetism*. London: Chapman and Hall.
- Thompson, R. and F. Oldfield 1986. *Environmental Magnetism*. London: Allen and Unwin.
- Turner, G. M. and R. Thompson 1982. Detransformation of the British geomagnetic secular variation record for Holocene times. *Geophys. J. R. Astr. Soc.* **70**, 789-792.